Acta Crystallographica Section A
Foundations of Crystallography
ISSN 0108-7673

Received 25 October 2010
Accepted 12 March 2011

Precession electron diffraction of Mn_2O_3 and $PbMnO_{2.75}$: solving structures where X-rays fail

Holger Klein

MCMF, Institut Néel, CNRS and University Joseph Fourier, 25 rue des Martyrs, BP 166, Grenoble, 38042, France. Correspondence e-mail: holger.klein@grenoble.cnrs.fr

The structure solutions of the two phases Mn_2O_3 and $PbMnO_{2.75}$ by precession electron diffraction (PED) are presented. In the powder samples used these structures could not be solved by X-ray diffraction because Mn_2O_3 is a minority phase in an MnO_2 powder and the complex structure of $PbMnO_{2.75}$ leads to severe peak overlap in the powder diffraction pattern. The influence of different parameters on the structure solution is studied, *i.e.* the number of reflections measured, precession angle, resolution limit and Lorentz-type correction. It is shown that the number of reflections is the most important parameter for successful structure solution from PED data.

1. Introduction

Electron crystallography has proven to be a powerful tool for structure solution. Many examples have been shown in which electron crystallography has been able to solve complex structures correctly (for recent examples, see ELCRYST, 2007; Gemmi & Nicolopoulos, 2007; Zou *et al.*, 2003). By combining electron crystallographic methods with X-ray powder diffraction, Baerlocher *et al.* (2007) and Gramm *et al.* (2006) have even solved complicated zeolite structures. The recent availability of the precession technique for electron diffraction has permitted unknown structures to be solved from electron diffraction data alone using standard crystallographic software (Boullay *et al.*, 2009; Mugnaioli *et al.*, 2009; Rozhdestvenskaya *et al.*, 2010; White *et al.*, 2010).

However, compared with X-ray crystallography it remains a delicate and time-consuming method. Therefore it finds its real application in cases where X-rays are not sufficient to solve the structures. Prominent examples are multiphase powders constituting nanometre-sized grains.

Here we present the structure solution of two samples where X-rays fail to solve the structure. The first one is a nanometre-sized powder of MnO_2, which is interesting for applications in batteries (Poinsignon *et al.*, 2006). This powder contained an impurity phase of low concentration, which we identified by electron diffraction to be α-Mn_2O_3. The α-Mn_2O_3 phase itself is not a very complex structure but in the present sample the X-ray powder diffraction peaks are masked by the main component of the powder, thus impeding the identification and structure solution of the impurity phase. We studied the influence of several parameters in the precession electron diffraction (PED) data acquisition and data treatment on the reliability of the results. The second sample is a pure powder of $PbMnO_{2.75}$. This complex structure suffers from severe peak overlap in the X-ray powder diffraction pattern and the cell parameters could not be determined by this technique. In a previous work we have determined the cation positions from the treatment of a high-resolution electron micrograph (HREM) (Klein, 2005). Here we present the structure as solved by PED.

2. Experimental

2.1. Samples

The Mn_2O_3 phase was found as an impurity in a nanocrystalline powder of β-MnO_2 synthesized by spray pyrolysis (Poinsignon *et al.*, 2006). A suspension of the powder in ethanol was agitated by ultrasound. Then a drop of the suspension was deposited on a copper grid covered by a holey amorphous carbon membrane for the transmission electron microscopy (TEM) study.

Fig. 1 shows a transmission electron micrograph of the secondary phase particle amongst clusters of MnO_2 crystals. The corresponding X-ray powder diffraction pattern (Poinsignon *et al.*, 2006) shows the expected peaks of the β-MnO_2 phase and a few additional peaks not consistent with this phase. However, these peaks are insufficient for a phase determination.

The $PbMnO_{2.75}$ phase was synthesized at 1153 K and 7.8 GPa. The structure has been determined, by Bougerol *et al.* (2002), to be monoclinic of space group $A2/m$ and with cell parameters a = 32.232, b = 3.831, c = 35.671 Å and β = 130°. The structure can be described as a superstructure of the perovskite containing crystallographic shear planes. The synthesized powder was crushed in an agate mortar and a suspension of the powder in ethanol was deposited on a holey carbon film for the TEM study.

2.2. Electron diffraction

Electron diffraction was performed using a Philips CM300ST operated at 300 kV and equipped with the 'spinning

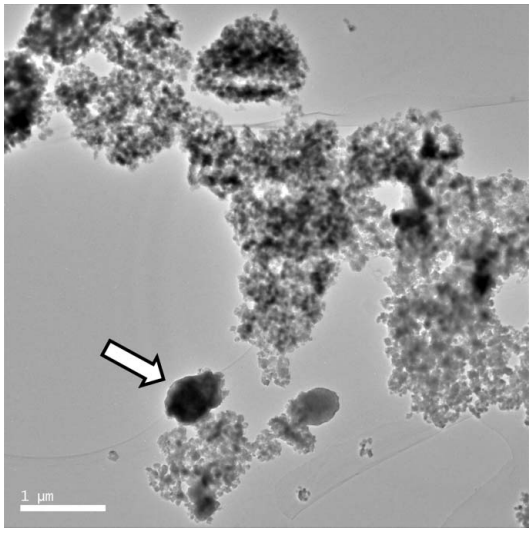

Figure 1
TEM micrograph showing clusters of MnO_2 crystals and a single particle of Mn_2O_3 (arrow).

star' precession device of Nanomegas (http://www.nanomegas.com/). Diffraction patterns were recorded using a GATAN Multiscan charge-coupled device (CCD) camera.

Selected area electron diffraction (SAED) was used to identify the minority phase in the MnO_2 powder as Mn_2O_3, which can be described in a cubic unit cell [space group $Ia\bar{3}$, a = 9.4 Å, Inorganic Crystal Structure Database (ICSD) No. 61271]. For the structure determination a total of 17 zone axes covering the asymmetrical unit were recorded under classical SAED conditions and in precession mode with different precession angles up to 4.1° (Fig. 2).

For each of these zone axes PED patterns were recorded with precession angles of 1.3, 2.4, 3.4 and 4.1°. Fig. 3 shows a comparison of the SAED pattern of the [111] zone axis with the PED patterns.

A single PED pattern of the [010] zone axis was recorded for $PbMnO_{2.75}$ with a precession angle of 2.4° (Fig. 4). This zone axis contains only reflections of the $h0l$ type. Therefore, only information about the x and z coordinates of the atoms can be obtained from this pattern. This is sufficient, however, since the y coordinate can be deduced by comparison with the related $PbMnO_3$ perovskite phase, the small b parameter and the space group allowing atoms to be located only at y = 0 or y = 0.5.

3. Data treatment

3.1. Mn_2O_3

The intensities of the reflections were extracted from the electron diffraction patterns (EDPs) using the *ELD* program of the *CRISP* package (http://www.calidris-em.com). Only reflections with $d > 0.8$ Å were retained for the structure determination. The intensities of equivalent reflections in each single EDP were merged using the program *Triple* (*CRISP*).

For each value of the precession angle the data obtained in the different zone axes of Mn_2O_3 were merged. After an additional merging of symmetry-equivalent reflections we obtained the intensities of 196 independent reflections in the complete data set stemming from the 17 zone axes.

Different data sets were obtained from these complete sets by retaining reflections only from selected zone axes (named Mxx, where xx denotes the number of zone axes included) and/or within a certain resolution limit. Table 1 gives the zone axes included in the different data sets considered. The data were either used as obtained from the diffraction patterns or they were corrected for the geometrical effects of the precession technique (Gemmi & Nicolopoulos, 2007). In the following this correction will be referred to as the Lorentz-type correction. No Lorentz-type correction was applied to the data sets with the smallest precession angle (1.3°) for which this correction is meaningless.

3.2. $PbMnO_{2.75}$

For $PbMnO_{2.75}$ all reflections with $d > 10$ Å, where the diffuse scattering around the transmitted beam gives considerable intensity, were ignored for the structure determination. This yielded a set of 1965 $h0l$ reflections, 991 of which were independent with a resolution limit of $d > 0.8$ Å. Again, different data sets were obtained by limiting the resolution to $d > 0.8$, $d > 1.0$ or $d > 1.2$ Å which contained 991, 682 and 473 independent reflections, respectively, and by applying or not the geometrical correction to each of these three sets.

4. Structure solution

The data sets were used as input for the *SIR2008* (http://www.ic.cnr.it/registration_form.php) program for structure determination using direct methods. The only parameters used in this structure determination that did not come directly from this work are the cell parameters, the space group and the number of atoms in the unit cell. These data were available from the literature, but could have been determined without difficulty from electron diffraction data and crystal chemistry considerations. For the purposes of this work we only considered the solution with the lowest R value proposed by *SIR2008*.

Since for both phases the quasi-kinematical approximation of $I \simeq F^2$ did not yield any reasonable structure solution, we assumed the measured intensities to be proportional to the structure-factor amplitude (Gemmi & Nicolopoulos, 2007).

5. Results

5.1. Mn_2O_3

The results of the structure solution using *SIR2008* for the different data sets are summarized in Table 2. For each of the data sets the table lists whether a correct solution of the structure was obtained. The eighth column shows the mean value over the different precession angles for the R factor of the correct solutions. The ratio of the height of the oxygen

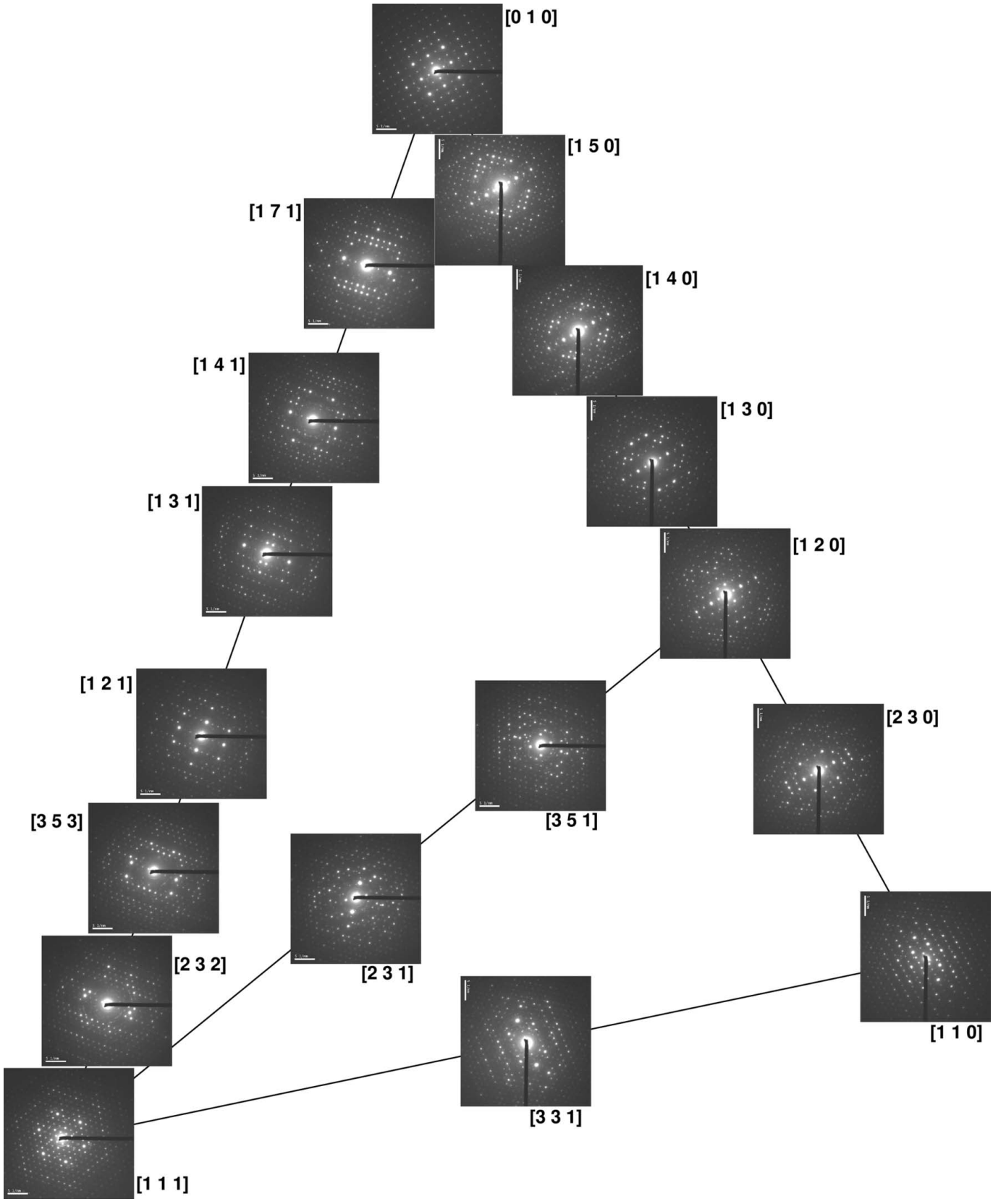

Figure 2
PED patterns of the 17 zone axes covering the asymmetric unit of the cubic cell of Mn_2O_3 obtained at a precession angle of 2.4°. In most patterns one can also observe reflections from the first-order Laue zone. Since they do not superimpose with the reflections of the zero-order Laue zone, they do not hinder the intensity determination.

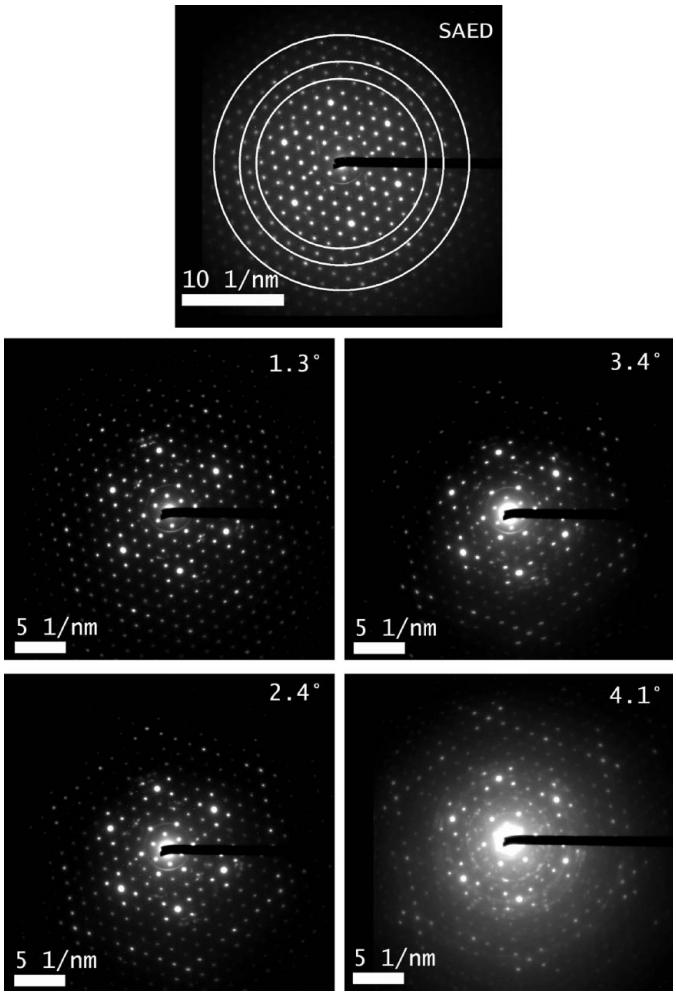

Figure 3
The SAED diffraction pattern (top) and PED patterns at different precession angles of the [111] zone axis of Mn_2O_3. The circles in the SAED pattern denote the resolution limits of 0.8, 1.0 and 1.2 Å.

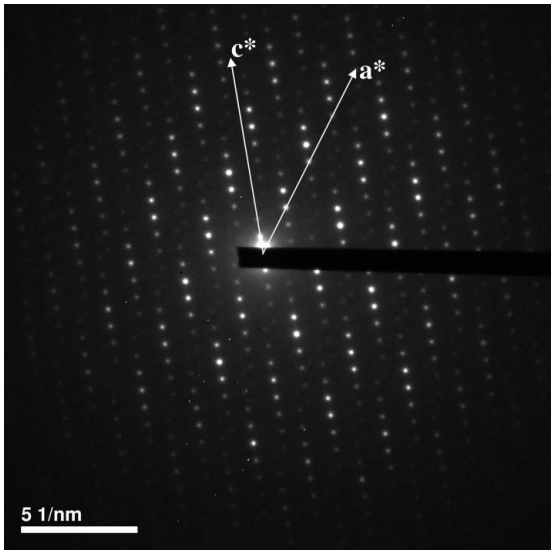

Figure 4
Electron diffraction pattern of the [010] zone axis of $PbMnO_{2.75}$. The a^* and c^* directions are indicated by arrows.

Table 1
Zone axes used in the different data sets and corresponding number of independent reflections.

The data sets are named M*xx*, where *xx* denotes the number of zone axes included.

Zone axis		M17	M8	M5	M3
[111]		×	×	×	×
[223]		×			
[335]		×			
[112]		×	×		
[113]		×	×	×	
[114]		×			
[117]		×			
[001]		×	×	×	×
[133]		×	×		
[011]		×	×	×	×
[023]		×			
[012]		×	×	×	
[013]		×	×		
[014]		×			
[015]		×			
[123]		×			
[135]		×			
No. of independent reflections	$d > 0.8$ Å	144	140	126	89
	$d > 1.0$ Å	75	75	71	55
	$d > 1.2$ Å	41	41	41	33

peak in the electron-density map with respect to the highest spurious peak is given as a measure of the noise level in the solution. The last two columns give the distances between the positions found in this work and the refined positions given in Table 3 from ICSD No. 61271 for the Mn2 and O1 atoms, respectively. The Mn1 atom is completely fixed by the symmetry of the crystal.

The observations that follow from Table 2 are the following.

(*a*) The most important parameter for obtaining a correct solution seems to be the number of reflections in the data set. The more reflections that are used, *i.e.* the more zone axes that are used and the higher the resolution limit, the more likely it is that a correct solution is obtained.

(*b*) The geometrical Lorentz-type correction does not influence significantly the possibility of obtaining a correct solution. The ratio of the oxygen peak height in the electron-density map to the spurious peaks is higher when the Lorentz-type correction is not applied.

(*c*) The *R* factors for all solutions are very close and in particular there is no correlation to the 'noise' (spurious peaks) in the electron-density map or to the precision of the obtained atom positions.

(*d*) The precession angle does not have a decisive influence except for the data sets containing few reflections. In these cases increasing the precession angle to over 2.5° does not improve the data quality; it may even deteriorate it (Eggeman *et al.*, 2010). This can possibly be attributed to the higher influence of the aberrations of the TEM lenses.

(*e*) The highest ratios $I_{\rm oxygen}/I_{\rm spurious}$ are obtained for the data sets containing 17 zone axes, and within the data sets containing the same number of zone axes the lowest ratio is found for the sets with a resolution limit of 1.2 Å. The ratios for those data sets to which the Lorentz-type correction was applied are lower than those for the non-corrected data sets.

Table 2
Results of the structure solution for the data sets containing different number of zone axes, the Lorentz-type correction, different resolution limits and precession angles.

The mean values of the *R* factors of the obtained solutions with different precession angles, and the ratio of the height of the oxygen peak to the highest spurious peak in the electron-density map are given. The mean distances of one Mn and the only O positions to the published positions are shown in the last columns, the other Mn position being completely fixed on its special position. 'OK' indicates that the correct structure was obtained whereas 'NA' denotes that no data were available.

No. of zone axes	Lorentz-type correction	Resolution limit (Å)	Precession angle				*R* factor	$I_{oxygen}/I_{spurious}$	Δ(Mn) (Å)	Δ(O) (Å)
			4.1°	3.4°	2.4°	1.3°				
17	No	1.2	OK	–	OK	OK	20%	2.3	0.10	0.20
17	No	1.0	OK	OK	OK	OK	20%	4.0	0.06	0.15
17	No	0.8	OK	OK	OK	OK	23%	3.3	0.04	0.10
17	Yes	1.2	OK	–	–	NA	14%	1.7	0.13	0.05
17	Yes	1.0	OK	OK	OK	NA	24%	2.9	0.10	0.07
17	Yes	0.8	OK	OK	OK	NA	27%	2.2	0.06	0.05
8	Yes	1.2	OK	–	OK	NA	27%	1.5	0.13	0.14
8	Yes	1.0	OK	OK	OK	NA	22%	1.8	0.11	0.06
8	Yes	0.8	OK	OK	OK	NA	27%	1.8	0.10	0.07
5	No	1.2	–	–	OK	OK	18%	2.6	0.03	0.10
5	No	1.0	–	–	OK	OK	23%	2.5	0.04	0.12
5	No	0.8	OK	OK	OK	OK	25%	2.8	0.07	0.11
5	Yes	1.2	–	OK	–	NA	32%	1.7	0.10	0.19
5	Yes	1.0	OK	–	OK	NA	23%	2.2	0.09	0.06
5	Yes	0.8	OK	OK	OK	NA	28%	2.4	0.10	0.07
3	No	1.2	–	–	–	OK	18%	1.1	0.06	0.24
3	No	1.0	OK	–	OK	OK	20%	1.2	0.14	0.20
3	No	0.8	OK	OK	–	OK	23%	1.3	0.06	0.22
3	Yes	1.2	–	–	–	NA	NA	NA	NA	NA
3	Yes	1.0	–	–	OK	NA	24%	1.1	0.05	0.05
3	Yes	0.8	–	–	OK	NA	24%	1.03	0.05	0.45

Table 3
Atom positions in the Mn_2O_3 structure (ICSD No. 61271).

Atom	Wyckoff position	*x*	*y*	*z*
Mn1	8*b*	1/4	1/4	1/4
Mn2	24*d*	−0.034	0	1/4
O1	48*e*	0.375	0.162	0.400

Table 4
Number of independent reflections and obtained *R* values as a function of the maximum resolution in $PbMnO_{2.75}$.

Resolution limit	Independent reflections	*R* value with Lorentz-type correction	*R* value without Lorentz-type correction
$d > 0.8$ Å	991	50%	42%
$d > 1.0$ Å	682	45%	38%
$d > 1.2$ Å	473	43%	36%

(*f*) There seems to be no correlation of the distances between the atom positions obtained in this study with the refined positions in the literature and either the number of zone axes, the application of the Lorentz-type correction or the resolution limit.

5.2. $PbMnO_{2.75}$

From the three data sets where the Lorentz-type correction was applied, only the one with a maximum resolution of 1.0 Å yielded a reasonable structure solution. The quality of this solution was the same as those of the solutions obtained without the Lorentz-type correction (*cf.* below). The other two data sets produced structures where large areas of the unit cell were empty. However, the difference in the quality of the obtained structures was not directly visible from the *R* values obtained (Table 4). In fact, the best solution did not correlate with the lowest *R* value. The *R* values decrease with decreasing resolution, which is to be expected from the fact that the number of reflections also decreases in this case.

When no Lorentz-type correction was applied to the data, all three data sets yielded the correct structure. Globally the *R* values were lower than in the previous case and again they decrease with a decreasing number of reflections.

All 29 independent cation positions were found with the 14 strongest peaks corresponding to the Pb atoms and the following 15 peaks to Mn as expected from their respective atom numbers. The next few peaks beyond peak number 30 correspond to oxygen positions in Bougerol *et al.* (2002). However, since not all peaks can be identified in the structural model we do not consider these positions here. Even though oxygen and other light atoms like lithium have recently been identified from PED data in some structures (Boullay *et al.*, 2009; Gemmi *et al.*, 2010), the presence of the heavy Pb atoms in a complex structure did not allow us to unambiguously identify the oxygen positions.

A comparison of the three solutions obtained without Lorentz-type correction shows that the structures are almost identical. Except for one Mn position in the 0.8 Å resolution data set the differences in the atom positions were at most 0.003. The mean distances between atom positions in the different solutions are therefore well below 0.1 Å.

In the structure determination of $PbMnO_{2.75}$ we used only one EDP corresponding to the [010] zone axis. Therefore all the measured reflections were of type *h*0*l* and no information on the atom positions along the *b* axis could be obtained. Consequently, the output of *SIR2008* gave for each atom a position of type *x*0*z*. Fig. 5 shows the projected structure obtained without Lorentz-type correction and with maximum resolution. Considering the small *b* parameter of the unit cell and the mirror plane perpendicular to **b** in the space group *A*2/*m*, the only possible values for *y* are $y = 0$ and $y = 0.5$.

Since we do not have experimental evidence that allows distinguishing between the two possibilities, we can only rely on a comparison with the crystal chemistry of the closely related perovskite-type structure $PbMnO_3$. The first position can be chosen freely since the resulting structures will be equivalent by an origin change of the unit cell. Once the position of the first cation is chosen, its next neighbours will be attributed the same *y* value if their projected distance onto the *ac* plane is close to 3.83 Å, and the *y* value will be increased by 0.5 if the projected distance is considerably smaller than this value.

In order to easily compare our results with the structure published by Bougerol *et al.* (2002) we have chosen the same *y* values as these authors. Table 5 gives the peak positions obtained from the data set without Lorentz-type correction and with a resolution limit of 0.8 Å, as well as the atom names given by Bougerol *et al.* (2002) and the distances between the published positions and our results.

Table 5
Atom positions obtained by PED for $PbMnO_{2.75}$ and comparison with the positions published by Bougerol *et al.* (2002).

The last column gives the distance between the positions in the two models.

Atom name	Wyckoff position	PED		Name in Bougerol *et al.* (2002)	X-ray diffraction		Δ (Å)
		x	*z*		*x*	*z*	
PB1	2*a*	0.000	0.000	Pb10	0	0	0.000
PB2	4*i*	0.942	0.068	Pb9	0.937	0.061	0.325
PB3	4*i*	0.150	0.120	Pb1	0.151	0.12	0.049
PB4	4*i*	0.678	0.086	Pb6	0.675	0.089	0.122
PB5	4*i*	0.209	0.053	Pb2	0.212	0.055	0.151
PB6	4*i*	0.737	0.018	Pb7	0.727	0.018	0.316
PB7	4*i*	0.472	0.035	Pb4	0.466	0.028	0.387
PB8	4*i*	0.414	0.102	Pb3	0.413	0.103	0.027
PB9	4*i*	0.886	0.137	Pb8	0.886	0.135	0.070
PB10	4*i*	0.620	0.152	Pb5	0.627	0.158	0.356
PB11	4*i*	0.358	0.172	Pb11	0.359	0.176	0.159
PB12	4*i*	0.093	0.188	Pb14	0.084	0.186	0.326
PB13	4*i*	0.170	0.295	Pb12	0.174	0.297	0.175
PB14	4*i*	0.432	0.276	Pb13	0.422	0.269	0.473
MN1	4*i*	0.050	0.103	Mn2	0.052	0.103	0.049
MN2	4*i*	0.261	0.160	Mn5	0.252	0.157	0.323
MN3	4*i*	0.841	0.047	Mn14	0.839	0.049	0.079
MN4	4*i*	0.787	0.122	Mn13	0.788	0.122	0.021
MN5	4*i*	0.523	0.140	Mn9	0.521	0.135	0.202
MN6	4*i*	0.313	0.084	Mn6	0.323	0.086	0.369
MN7	4*i*	0.577	0.066	Mn10	0.578	0.057	0.300
MN8	4*i*	0.368	0.010	Mn7	0.36	0.004	0.378
MN9	4*i*	0.996	0.178	Mn1	0.992	0.172	0.280
MN10	4*i*	0.696	0.261	Mn11	0.69	0.26	0.207
MN11	4*i*	0.104	0.028	Mn3	0.102	0.017	0.410
MN12	4*i*	0.733	0.196	Mn12	0.725	0.194	0.271
MN13	4*i*	0.470	0.214	Mn8	0.475	0.205	0.303
MN14	4*i*	0.957	0.244	Mn15	0.952	0.243	0.196
MN15	4*i*	0.211	0.231	Mn4	0.226	0.228	0.452

6. Discussion

6.1. Mn_2O_3

From the systematic study of the influence of the different experimental parameters and the data treatment, it is clear that a large number of reflections is an important asset for obtaining a correct structure model. Increasing the number of independent reflections either by increasing the number of zone axes or by increasing the resolution limit leads to a better probability for solving the structure regardless of the other parameters (precession angle, application of the Lorentz-type correction). Table 2 shows that the M3 data sets never solve the structure with a resolution limit of 1.2 Å. Data sets with more zone axes solve the structure with a resolution limit of 0.8 Å for all precession angles, while the probability of solving the structure with other resolution limits increases with the number of zone axes used.

In addition to the increase of the number of independent reflections, an increase in the redundancy of the data helps identify the correct structure. Calculating the mean value for the intensities obtained from different zone axes not only reduces the statistical errors but also decreases the impact of systematic errors (*e.g.* dynamical diffraction effects) that might be present in one zone axis but not the others.

Comparing the ratio of the intensities of the oxygen peaks in the electron-density map with the spurious peaks, one can see that this ratio is higher for the data sets containing 17 zone axes than for those containing only five zone axes, although the number of independent reflections is similar in both cases.

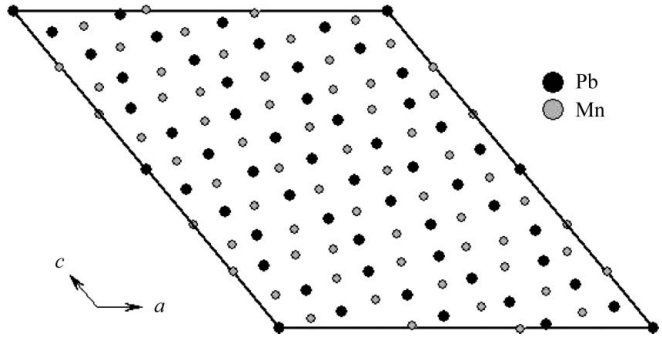

Figure 5
Projection of the structure of $PbMnO_{2.75}$ obtained from PED without Lorentz-type correction and with maximum resolution.

The higher ratio leads to electron-density maps where the correct peaks are identified more easily.

6.2. $PbMnO_{2.75}$

The distances between the obtained positions and those found by refinement against X-ray powder diffraction data are given in the last column of Table 5. The mean distance for Pb atoms is 0.21 Å; for Mn atoms it is 0.26 Å. These values show a good agreement between the two models, especially when taking into account the standard deviation of the result of the X-ray refinement of 0.1 Å for Pb and 0.3 Å for Mn.

Finally, the oxygen positions can be determined in accordance with the crystal chemistry of the perovskite phases. In the closely related phase $PbMnO_3$ the Mn atoms are in the centre of oxygen octahedra. In the *b* direction the oxygen are located at $y_{Mn} + 0.5$ and in the *ac* plane the missing O atoms are placed half way between the Mn atoms.

In this way a model of the complete structure can be obtained. The atom positions are close to the real values and without a doubt close enough to refine the positions. Since the *R* value of the structure solution of the electron diffraction data is rather high ($R = 0.42$), it is not reasonable to refine the positions with these data. A refinement of the positions using X-ray powder diffraction data will, however, certainly enhance the accuracy of the model.

For the two structures presented here the application of the geometrical Lorentz-type correction for the PED data leads to poorer results than those obtained from the non-corrected data. The Lorentz-type correction consists of multiplying the measured intensities by a factor that increases with increasing diffraction angle in order to compensate for the smaller time these reflections are in the Bragg condition during the precession movement of the incident beam. Although it is clear that in kinematical diffraction this purely geometric correction has to be applied in order to obtain correct data, in PED the situation may depend on the experimental conditions. In not too thin samples, even though the precession technique greatly reduces multiple diffraction, it is not completely removed. One of the effects of this multiple diffraction is, on average, to transfer intensity from reflections at low angles to reflections further away from the transmitted beam. In this way the remaining multiple diffraction 'mimics' the Lorentz-type correction and applying the Lorentz-type correction on top of this might 'overcorrect' the data.

7. Conclusion

Two examples of very different phases in very different samples show that precession electron diffraction can be used to solve the structures of crystals. In the present examples we have shown that electron crystallography cannot only be applied to samples where the structures can be solved by X-ray diffraction but also in cases where X-ray structure determination fails. The most important experimental parameter for obtaining a correct solution is the number of measured reflections used in the structure solution.

References

Baerlocher, C., Gramm, F., Massüger, L., McCusker, L. B., He, Z., Hovmöller, S. & Zou, X. (2007). *Science*, **315**, 1113–1116.

Bougerol, C., Gorius, M. F. & Grey, I. E. (2002). *J. Solid State Chem.* **169**, 131–138.

Boullay, P., Dorcet, V., Pérez, O., Grygiel, C., Prellier, W., Mercey, B. & Hervieu, M. (2009). *Phys. Rev. B*, **79**, 184108.

Eggeman, A. S., White, T. A. & Midgley, P. A. (2010). *Ultramicroscopy*, **110**, 771–777.

ELCRYST (2007). *Ultramicroscopy*, **107**, 431–558.

Gemmi, M., Klein, H., Rageau, A., Strobel, P. & Le Cras, F. (2010). *Acta Cryst.* B**66**, 60–68.

Gemmi, M. & Nicolopoulos, S. (2007). *Ultramicroscopy*, **107**, 483–494.

Gramm, F., Baerlocher, C., McCusker, L. B., Warrender, S. J., Wright, P. A., Han, B., Hong, S. B., Liu, Z., Ohsuna, T. & Terasaki, O. (2006). *Nature (London)*, **444**, 79–81.

Klein, H. (2005). *Philos. Mag. Lett.* **85**, 569–575.

Mugnaioli, E., Gorelik, T. & Kolb, U. (2009). *Ultramicroscopy*, **109**, 758–765.

Poinsignon, Chr., Djurado, E., Klein, H., Strobel, P. & Thomas, F. (2006). *Electrochim. Acta*, **51**, 3076–3085.

Rozhdestvenskaya, I., Mugnaioli, E., Czank, M., Depmeier, W., Kolb, U., Reinholdt, A. & Weirich, T. (2010). *Miner. Mag.* **74**, 159–177.

White, T. A., Moreno, M. S. & Midgley, P. A. (2010). *Z. Kristallogr.* **225**, 56–66.

Zou, X. D., Mo, Z. M., Hovmöller, S., Li, X. Z. & Kuo, K. H. (2003). *Acta Cryst.* A**59**, 526–539.